

REPORT

CATALYSIS

Active sites for CO₂ hydrogenation to methanol on Cu/ZnO catalysts

Shyam Kattel,¹ Pedro J. Ramírez,² Jingguang G. Chen,^{1,3*}
José A. Rodriguez,^{1,4*} Ping Liu^{1,4*}

The active sites over commercial copper/zinc oxide/aluminum oxide (Cu/ZnO/Al₂O₃) catalysts for carbon dioxide (CO₂) hydrogenation to methanol, the Zn-Cu bimetallic sites or ZnO-Cu interfacial sites, have recently been the subject of intense debate. We report a direct comparison between the activity of ZnCu and ZnO/Cu model catalysts for methanol synthesis. By combining x-ray photoemission spectroscopy, density functional theory, and kinetic Monte Carlo simulations, we can identify and characterize the reactivity of each catalyst. Both experimental and theoretical results agree that ZnCu undergoes surface oxidation under the reaction conditions so that surface Zn transforms into ZnO and allows ZnCu to reach the activity of ZnO/Cu with the same Zn coverage. Our results highlight a synergy of Cu and ZnO at the interface that facilitates methanol synthesis via formate intermediates.

The leading catalysts currently used in industry for hydrogenation of CO₂ to methanol (CO₂ + 3H₂ → CH₃OH + H₂O) (1–3) are Cu/ZnO/Al₂O₃. The efforts to understand the nature of active sites in Cu/ZnO (4–7) have led to debate about the role of ZnO (8). One possibility is that there is an intimate synergy between Cu and ZnO at the interface, where ZnO could act as a structural modifier, hydrogen reservoir, or direct promoter for bond activation (4, 9–11). The other possibility is that a highly active ZnCu alloy forms by partial reduction of ZnO or a decoration of Cu with metallic Zn (5, 6, 12–14).

Although a recent experiment observed higher activity of ZnCu silicate than Cu/ZnO (7), little was known about the sites on the top layer of the system that catalyzed the overall reaction due to the limitations in experimental techniques. To describe the active sites on the surface, theoretical calculations were carried out to provide mechanistic understanding of methanol synthesis from CO₂ on either Cu/ZnO(0001) (15) or Zn-decorated Cu(211) step edges (5, 16). Furthermore a recent transmission electron microscopy (TEM) study revealed the formation of a ZnO overlayer on top of the Cu particles in an industrial Cu/ZnO/Al₂O₃ catalyst under reaction conditions (4) that could form a catalytically active metal-oxide interface (17).

Here, we report a direct comparison of ZnCu and ZnO/Cu model catalysts during CO₂ hydro-

genation to methanol using a combination of x-ray photoelectron spectroscopy (XPS) measurements, density functional theory (DFT) calculations, and kinetic Monte Carlo (KMC) simulations. Experimentally, Cu(111), ZnCu(111), ZnO/Cu(111), Cu/ZnO(0001), and ZnO/Cu/ZnO(0001) model systems were synthesized for systematic comparison. Theoretically, the direct mechanistic comparison between ZnCu(211), an active phase for ZnCu alloy identified previously (5), and ZnO/Cu(111) was made. In this way, the experiments on well-characterized model surfaces can be strongly coupled with the theoretical calculations, which provides more insight into the active sites than the previous experiment-theory combined studies on methanol synthesis over Cu/ZnO catalysts (5, 6, 16).

The ZnCu(111) and ZnO/Cu(111) model surfaces were synthesized (18) to simulate ZnCu alloy and the inverse ZnO/Cu motif observed previously with TEM (4–6). For the clean Cu(111) substrate, under a pressure of 4.5 atm of H₂ and 0.5 atm of CO₂ at 575 K, a turnover frequency (TOF) was determined for the synthesis of methanol of 0.006 molecules site⁻¹ s⁻¹, which is near the value of 0.008 reported for polycrystalline copper and smaller by a factor of 5 than the value of 0.032 molecules site⁻¹ s⁻¹ reported for Cu(110), under similar conditions (19). This result is consistent with the hypothesis that the more open Cu(110) surface is more active than Cu(111) (19). In all cases, very low methanol yields were observed on Cu(111) (0.1×10^{13} to 1.1×10^{13} CH₃OH molecules cm⁻² s⁻¹). As shown in Fig. 1A, the catalytic activity increased after ZnO was deposited on the copper substrate, which reached a maximum at ~0.2 monolayer (ML) and then decreased with the increasing ZnO coverage, similar to the behavior seen upon deposition of this oxide on polycrystalline copper (20). Thus, the exposure of both

ZnO and Cu sites or the optimization of the ZnO-Cu interfacial site is required to enhance the methanol production. During the hydrogenation of CO₂, a large amount of CO is produced through the reverse water-gas shift (RWGS) reaction (19, 20). For the production of CO (fig. S1), the same trends were found as for the CO₂ → methanol conversion. After depositing ZnO nanoparticles (NPs) on Cu(111), the reaction rates were 5 to 18 times as fast as that reported on the most reactive surface of copper, Cu(110) (19).

The as-prepared ZnO/CuO_x/Cu(111) systems (18) were transformed into ZnO/Cu(111) after reaction. Figure S2 shows the typical Zn 2p_{3/2} XPS spectra collected after reaction, and the measured peak position is near 1021.6 eV. The range for Zn²⁺ is 1021.6 to 1021.7 eV, and that for Zn⁰ is 1021.1 eV (20, 21). Thus, under a CO₂/H₂ reaction feed that was rich in H₂, the ZnO/Cu system was stable, and no sign was seen for a ZnO/Cu → ZnCu transformation. We exposed the ZnO/Cu(111) catalysts to 20 atm of H₂ at the typical temperatures used for methanol production, and after evacuation of the gas without exposure to air, we did not detect any reduction of ZnO in the XPS measurements.

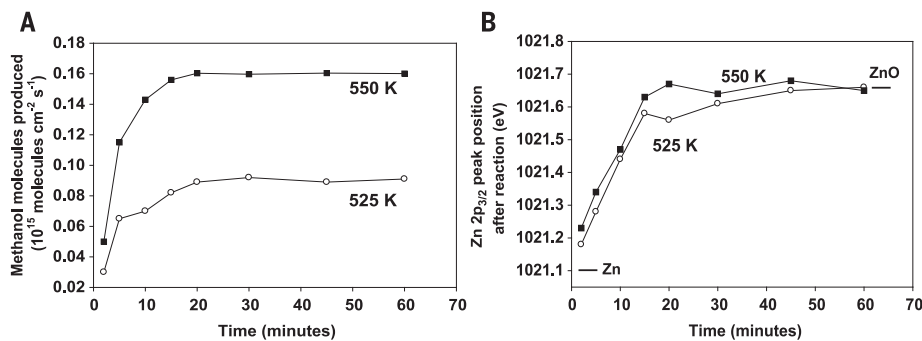
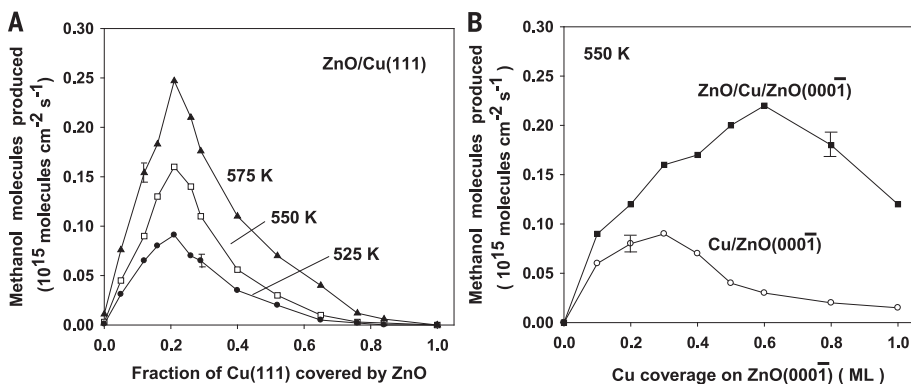
Our studies indicated that the ZnCu(111) surfaces were not stable under reaction conditions as Zn eventually transformed into ZnO. This result is consistent with a previous study for Zn on polycrystalline copper (20). As shown in Fig. 2A, at both 525 and 550 K, the activity of Cu(111) precovered by 0.2 ML of Zn was initially low and increased with time until reaching values that matched those reported in Fig. 1A for 0.2 ML of ZnO on Cu(111). According to the XPS measurements in Fig. 2B, such activity variation was accompanied by the shift in the corresponding Zn 2p_{3/2} peak positions measured after a given reaction time, evolving from a binding energy of ~1021.1 eV (Zn) to 1021.65 eV (ZnO). The Zn → ZnO transformation was accompanied by an increase in the catalytic activity for methanol production, and the optimal composition for CO₂ conversion to methanol was ZnO/Cu(111).

We also investigated the CO₂ → methanol conversion on the model Cu/ZnO(0001) and ZnO/Cu/ZnO(0001) catalysts. The Cu/ZnO(0001) catalysts were prepared following the methodology described in (22). Copper grows on the O-terminated (0001) face of ZnO to form two-dimensional (2D) particles at low coverages (<0.15 ML) and 3D particles at high coverages (23). Figure 1B shows the results for the production of methanol on Cu/ZnO(0001) at 550 K. The clean ZnO surface was not active until Cu was present. Small particles of Cu deposited on ZnO(0001) were the most active because of the higher concentration of corner or edge atoms. The best Cu/ZnO(0001) catalyst in Fig. 1B exhibited a lower activity than the best ZnO/Cu(111) inverse catalyst in Fig. 1A.

The presence of ZnO NPs likely facilitated the ZnO-Cu interactions. To obtain this type of interaction, and to mimic the ZnO/Cu/ZnO configuration observed with the TEM images for powder catalysts (4), we vapor-deposited 0.4 ML of ZnO onto the Cu/ZnO(0001) surface. The deposited

¹Chemistry Division, Brookhaven National Laboratory, Upton, NY 11973, USA. ²Facultad de Ciencias, Universidad Central de Venezuela, Caracas 1020-A, Venezuela. ³Department of Chemical Engineering, Columbia University, New York, NY 10027, USA. ⁴Department of Chemistry, State University of New York-Stony Brook, Stony Brook, NY 11790, USA.

*Corresponding author. Email: jgchen@columbia.edu (J.G.C.); rodrigez@bnl.gov (J.A.R.); pingliu3@bnl.gov (P.L.)



ZnO likely landed on both the ZnO(0001̄) substrate and the Cu NPs to form inverse oxide/metal catalysts. A large increase in catalytic activity and the shift of the maximum to the high Cu coverage occurred when going from Cu/ZnO(0001̄) to ZnO/Cu/ZnO(0001̄) (Fig. 1B), demonstrating the importance of inverse systems and the presence of an active ZnO-Cu interface for methanol synthesis on Cu/ZnO catalysts. After exposing the most active ZnO/Cu/ZnO(0001̄) catalysts to 20 atm of H₂ at 525 to 575 K in a high-pressure reactor, we found no sign of ZnO reduction in the post-reaction XPS measurements.

To gain further mechanistic understanding of methanol synthesis from CO₂ on the ZnCu(111) and ZnO/Cu(111) model catalysts, DFT calculations (18) were performed on ZnCu(211) (Fig. 3A) to describe ZnCu alloys (5) and Zn₆O₇H₇/Cu(111) (Fig. 3B) to model the ZnO-Cu interface (3). Following previous studies (3, 5, 22, 24–26), two main reaction pathways for CO₂ conversion to methanol were considered in our calculations: (i) The RWGS reaction to produce a CO intermediate followed

by its hydrogenations to methanol (RWGS + CO-hydro pathway) and (ii) initial hydrogenation of CO₂ to a *HCOO intermediate followed by its hydrogenation and dissociation to methanol (formate pathway).

In agreement with previous calculations (5), the present DFT results also show the slightly preferred formate pathway on ZnCu(211) via *HCOOH, *H₂COOH, and *CH₃O intermediates over the RWGS + CO-hydro pathway for methanol synthesis (Fig. 3A). Herein, CO₂ hydrogenation may proceed through an Eley-Rideal (ER) mechanism, as is the case for pure Cu catalysts (27) due to the unfavorable CO₂ binding at the Zn-Cu hybrid site (fig. S3 and table S1). CO is expected to be the main product along the RWGS + CO-hydro pathway, and only a small amount of *HCO can be further hydrogenated to *CH₃OH, as is that along the formate pathway. In addition, the current calculations also included the direct dissociation of *CO₂ to *CO + *O. The strong oxygen affinity of Zn sites makes the *O formation more kinetically favorable than hydrogenation to *HCOO

[activation energy (E_a) = 0.99 eV] and competitive with its hydrogenation to *HCOO (E_a = 0.77 eV). Because the hydrogenation of *O at the Zn sites to *OH (E_a = 1.21 eV) is rather difficult, *O species are likely to be stabilized on the surface and lead to the formation of a ZnO layer during the CO₂ hydrogenation reaction, as was seen in the experiments for ZnCu(111) (Fig. 2A).

On ZnO/Cu(111), the stabilization of reaction intermediates involved in CO₂ hydrogenation requires Cu, Zn, or the synergy of both sites, and the ZnO-Cu interface likely provides multiple active sites for the reaction (fig. S4). CO₂ is activated in a similar way on ZnO/Cu(111) (Fig. 3B) as that on ZnCu(211) (Fig. 3A). Again the formate pathway likely dominates for CO₂ hydrogenation to methanol. Along the RWGS + CO-hydro pathway, although CO is still the major product, desorption is more favorable than on ZnCu(211) because of weakened CO binding and hindered hydrogenation to *HCO (tables S1 and S2).

The results from our KMC simulations under the experimental conditions (18) were consistent with the DFT predictions, showing that CO₂ hydrogenation favored the formate pathway on both systems. On pure Cu catalysts, *HCOO species are identified as only spectators for methanol synthesis (28). For both ZnCu and ZnO/Cu systems, the addition of Zn or ZnO helps in stabilizing the *HCOOH intermediates via direct Zn-O interaction (figs. S3 and S4) and in activating *HCOO via hydrogenation. The rate for the methanol production on ZnCu(211) is very low and quickly decays (Fig. 4A). First, the low conversion rate is associated with the activated hydrogenations of *HCOO to *HCOOH (E_a = 1.19 eV). In addition, the reverse reaction, *H + *HCOO → *HCOOH, is more facile (E_a = 0.50 eV) than the forward reaction. Thus, the *HCOOH intermediate is not stable but decomposes back to *HCOO. As a result, the strongly bound *HCOO species occupy the surface sites (Fig. 4B), in agreement with the previous XPS study and DFT calculations (16, 20). Furthermore, the production of methanol is also hindered by *H₃CO hydrogenation to *CH₃OH (E_a = 1.49 eV), although the accumulation of *H₃CO is not as much as that of *HCOO (Fig. 4B). The strong binding of *HCOO and *H₃CO with the surface likely poisons the catalyst, and the production of methanol decreases over time (Fig. 4A).

The accumulation of *O species (Fig. 4B) is associated with *CO₂ dissociation to *CO + *O at the Zn sites of ZnCu(211) and is facilitated by the high activation barrier to hydrogenation to *OH (E_a = 1.21 eV), leading to the transformation of Zn to ZnO. The combination of ZnO and Cu leads to a steady methanol production at a rate much greater than that on ZnCu(211) (Fig. 4A). The *O species on ZnCu(211) are promoters instead of surface poisoning agents in this case. Accordingly, the methanol production rate (Fig. 4A) for ZnCu(211) likely increases to the level observed on ZnO/Cu due to the formation of *O and ZnO after ~900 s (Fig. 4B).

The enhanced methanol production on ZnO/Cu(111) is attributed to the facile key elementary

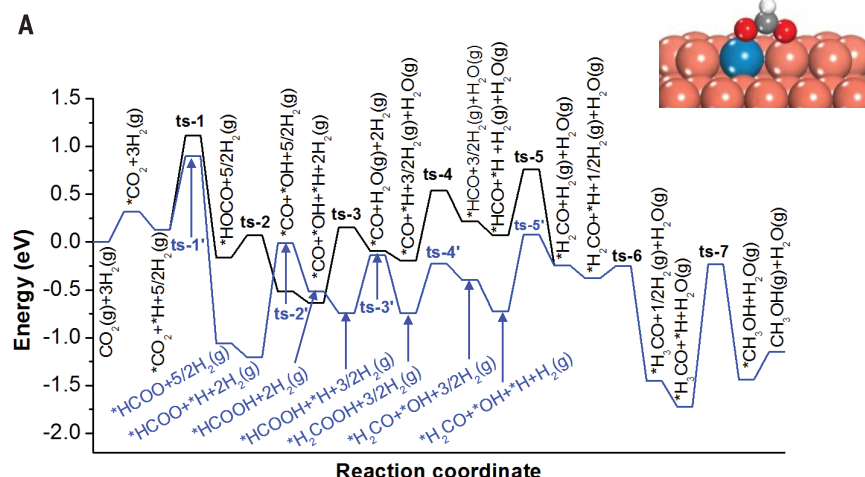
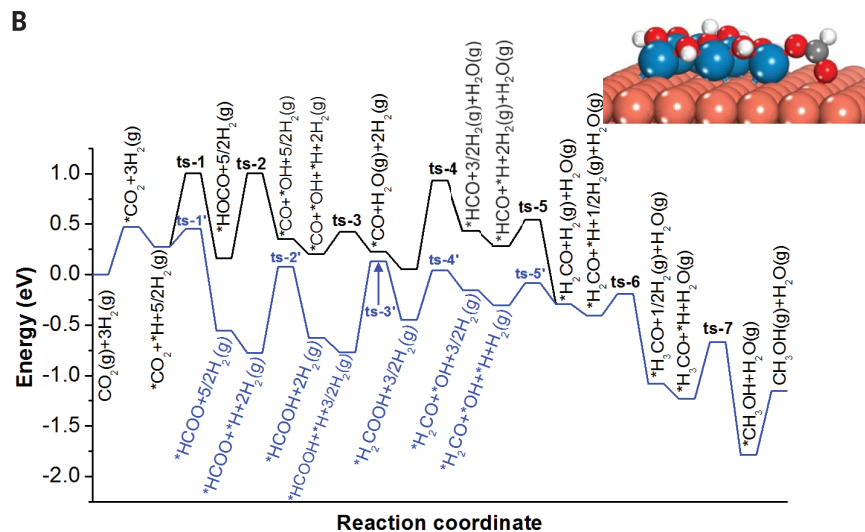
A**B**

Fig. 3. Potential energy diagram. Potential energy diagram for the hydrogenation of $\text{CO}_2(\text{g})$ to $\text{CH}_3\text{OH}(\text{g})$ on (A) ZnCu(211) and (B) ZnO/Cu(111) via the RWGS + CO-hydro and formate pathways. ts, transition state. (Inset) Structures of $^*\text{HCOO}$ on ZnCu(211) (A) and ZnO/Cu(111) (B). Cu, brown; Zn, blue; O, red; H, white; C, gray.

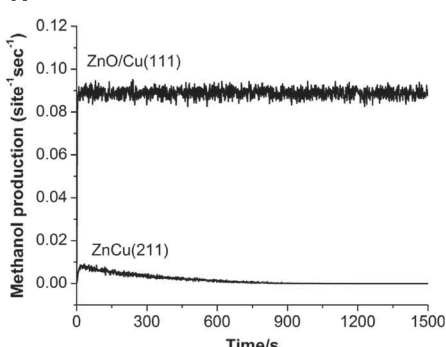
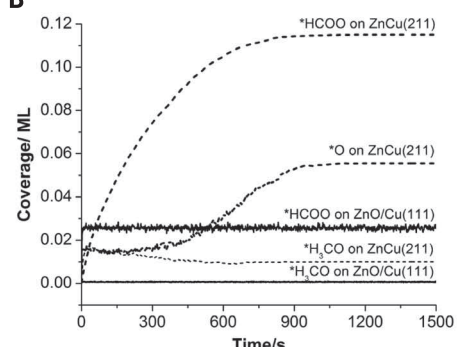
A**B**

Fig. 4. KMC simulations for CO_2 hydrogenation. (A) Rate of methanol production on ZnCu(211) and ZnO/Cu(111) at 525 K and ratio of partial pressure of H_2 and CO_2 ($P_{\text{H}_2}/P_{\text{CO}_2}$) of 9:1. (B) Coverage of surface reaction intermediates on ZnCu(211) and ZnO/Cu(111) under reaction conditions.

steps. For CO_2 hydrogenation to methanol on ZnO/Cu(111), the hydrogenation of $^*\text{H}_3\text{CO}$ is no longer rate-controlling ($E_a = 0.56$ eV), as is that on ZnCu(211). The bottleneck is associated with $^*\text{HCOO}$ ($E_a = 0.85$ eV) and $^*\text{HCOOH}$ ($E_a = 0.90$ eV) hydrogenation reactions, and the corresponding barriers are much lower than that on ZnCu(211) ($E_a = 1.49$ eV). Only $^*\text{HCOO}$ species are also observed on the ZnO/Cu(111) surface, and the total amount of occupied sites is lower than that on ZnCu(211) (Fig. 4B) because of the bond-weakening introduced by a transformation from Zn to ZnO (table S1). In addition, the identified active ZnO-Cu interface in DFT also explains the volcano trend between methanol production and ZnO coverage on Cu(111) (Fig. 1A). Such observation also agrees well with the previous studies, showing that the high methanol synthesis activity is associated with the combination of Cu and ZnO NPs (6, 29, 30). Accordingly, the previously observed increase in methanol production with the formation of ZnCu (5, 6, 12–14, 31) is likely attributed to the well dispersion of Zn sites, and therefore ZnO, on the top layer of the copper surface under reaction conditions, resulting in an increase in the active ZnO-Cu sites and eventual methanol production.

REFERENCES AND NOTES

- M. D. Porosoff, B. H. Yan, J. G. G. Chen, *Energy Environ. Sci.* **9**, 62–73 (2016).
- J. A. Rodriguez et al., *ACS Catal.* **5**, 6696–6706 (2015).
- J. Graciani et al., *Science* **345**, 546–550 (2014).
- T. Lunknenbein, J. Schumann, M. Behrens, R. Schlögl, M. G. Willinger, *Angew. Chem. Int. Ed.* **54**, 4544–4548 (2015).
- M. Behrens et al., *Science* **336**, 893–897 (2012).
- S. Kuld et al., *Science* **352**, 969–974 (2016).
- R. van den Berg et al., *Nat. Commun.* **7**, 13057 (2016).
- M. Behrens, *Angew. Chem. Int. Ed.* **55**, 14906–14908 (2016).
- S. A. Kondrat et al., *Nature* **531**, 83–87 (2016).
- M. Behrens et al., *Chem. Cat. Chem.* **2**, 816–818 (2010).
- O. Martin et al., *Angew. Chem. Int. Ed.* **55**, 11031–11036 (2016).
- S. Kuld, C. Conradsen, P. G. Moses, I. Chorkendorff, J. Sehested, *Angew. Chem. Int. Ed.* **53**, 5941–5945 (2014).
- J. Nakamura, Y. Choi, T. Fujitani, *Top. Catal.* **22**, 277–285 (2003).
- J. D. Grunwaldt, A. M. Molenbroek, N. Y. Topsøe, H. Topsøe, B. S. Clausen, *J. Catal.* **194**, 452–460 (2000).
- L. Martinez-Suárez, N. Siemer, J. Frenzel, D. Marx, *ACS Catal.* **5**, 4201–4218 (2015).
- F. Studt et al., *ChemCatChem* **7**, 1105–1111 (2015).
- V. Schott et al., *Angew. Chem. Int. Ed.* **52**, 11925–11929 (2013).
- Materials and methods are available as supplementary materials.
- J. Yoshihara, C. T. Campbell, *J. Catal.* **161**, 776–782 (1996).
- J. Nakamura et al., *J. Catal.* **160**, 65–75 (1996).
- C. T. Campbell, K. A. Daube, J. M. White, *Surf. Sci.* **182**, 458–476 (1987).
- Y. Yang, J. Evans, J. A. Rodriguez, M. G. White, P. Liu, *Phys. Chem. Chem. Phys.* **12**, 9909–9917 (2010).
- L. V. Kopitz, O. Dulub, U. Diebold, *J. Phys. Chem. B* **107**, 10583–10590 (2003).
- L. C. Grabow, M. Mavrikakis, *ACS Catal.* **1**, 365–384 (2011).
- S. Kattel, B. Yan, Y. Yang, J. G. Chen, P. Liu, *J. Am. Chem. Soc.* **138**, 12440–12450 (2016).
- S. Posada-Pérez et al., *J. Am. Chem. Soc.* **138**, 8269–8278 (2016).
- H. Nakano, I. Nakamura, T. Fujitani, J. Nakamura, *J. Phys. Chem. B* **105**, 1355–1365 (2001).
- Y. Yang, D. Mei, C. H. F. Peden, C. T. Campbell, C. A. Mims, *ACS Catal.* **5**, 7328–7337 (2015).

29. F. Liao *et al.*, *Angew. Chem. Int. Ed.* **50**, 2162–2165 (2011).
 30. M. B. Fichtl *et al.*, *Angew. Chem. Int. Ed.* **53**, 7043–7047 (2014).
 31. C. Tisseraud, C. Comminges, S. Pronier, Y. Pouilloux, A. Le Valant, *J. Catal.* **343**, 106–114 (2016).

ACKNOWLEDGMENTS

The research was carried out at Brookhaven National Laboratory (BNL) supported by the U.S. Department of Energy (DOE), Office of Science, Office of Basic Energy Sciences, Division of

Chemical Sciences, Biosciences and Geosciences, under contract DE-SC0012704. The DFT calculations were performed using computational resources at the Center for Functional Nanomaterials at BNL, a DOE Office of Science User Facility, and at the National Energy Research Scientific Computing Center (NERSC), a DOE Office of Science User Facility, supported by the Office of Science of the DOE under contract DE-AC02-05CH11231. All data needed to evaluate the conclusions are presented in the paper and supplementary materials.

SUPPLEMENTARY MATERIALS

www.scienmag.org/content/355/6331/1296/suppl/DC1
 Materials and Methods
 Supplementary Text
 Figs. S1 to S4
 Tables S1 to S3
 References (32–48)

7 November 2016; resubmitted 23 January 2017
 Accepted 23 February 2017
[10.1126/science.aal3573](https://doi.org/10.1126/science.aal3573)

Active sites for CO₂ hydrogenation to methanol on Cu/ZnO catalysts

Shyam Kattel, Pedro J. Ramírez, Jingguang G. Chen, José A. Rodriguez and Ping Liu (March 23, 2017)

Science **355** (6331), 1296-1299. [doi: 10.1126/science.aal3573]

Editor's Summary

Metal-oxide synergy

The hydrogenation of carbon dioxide is a key step in the industrial production of methanol. Catalysts made from copper (Cu) and zinc oxide (ZnO) on alumina supports are often used. However, the actual active sites for this reaction—Zn-Cu bimetallic sites or ZnO-Cu interfacial sites—are debated. Kattel *et al.* studied model catalysts and found that ZnCu became as active as ZnO/Cu only after surface oxidation formed ZnO. Theoretical studies favor a formate intermediate pathway at a ZnO-Cu interface active site.

Science, this issue p. 1296

This copy is for your personal, non-commercial use only.

Article Tools Visit the online version of this article to access the personalization and article tools:
<http://science.scienmag.org/content/355/6331/1296>

Permissions Obtain information about reproducing this article:
<http://www.scienmag.org/about/permissions.dtl>